PERGAMON

International Journal of Heat and Mass Transfer 45 (2002) 4045–4055

International Journal of HEAT and MASS TRANSFER

www.elsevier.com/locate/ijhmt

Modeling heat and moisture transfer through fibrous insulation with phase change and mobile condensates

Jintu Fan [a,*], Xinghuo Wen [b]

[a] *Institute of Textiles and Clothing, The Hong Kong Polytechnic University, Hung Hom, Kowloon, Hong Kong*
[b] *Lab and Equipment Division, Tsinghua University, Beijing 100084, China*

Received 6 April 2001; received in revised form 10 November 2001

Abstract

This paper reports on a transient model of coupled heat and moisture transfer through fibrous insulation, which for the first time takes into account of evaporation and mobile condensates. The model successfully explained the experimental observations of Farnworth [Tex. Res. J. 56 (1986) 653], and the numerical results of the model were found to be in good agreement with the experimental results of a drying test. Based on this model, numerical simulation was carried out to better understand the effect of various material and environmental parameters on the heat and moisture transfer. It was found that the initial water content and thickness of the fibrous insulation together with the environmental temperature are the three most important factors influencing the heat flux. © 2002 Elsevier Science Ltd. All rights reserved.

Keywords: Heat and moisture transfer; Water evaporation; Numerical simulation

1. Introduction

Condensation in fibrous insulation is a serious problem in clothing and many other applications such as building insulation and refrigerated space envelopes, as it can result in drastic reduction in thermal insulation of the system.

Despite of the vast published work on heat and moisture transfer in fibrous insulation, little has been done on the coupled heat and moisture transfer with phase change until 1980s. Ogniewicz and Tien [1] are the first workers who have contributed the subject through theoretical modelling and numerical analysis, assuming heat is transported by conduction and convection and the condensate is in pendular state. The analysis was limited to a quasi-steady-state, viz. the temperature and vapor concentration remain unchanged with time before the condensates become mobile. Motakef and El-Masri [2] first considered the quasi-steady-state corresponding to mobile condensate, and presented an approximate solution by neglecting the condensation during the initial transient period and effects of condensate motion on the temperature distribution. This theoretical model was later extended by Shapiro and Motakef [3] to analyze the unsteady heat and moisture transport processes through the calculation of quasi-steady fields in time-varying domains and compared the analytical results with experimental ones under some very limited circumstances. This analysis was only appropriate when the time scale for the motion of the dry-wet boundary in porous media is much larger than the thermal diffusion time scale, which may however not be the case with frosting and small moisture accumulation [4].

Farnworth [5] presented the first dynamic model of coupled heat and moisture transfer with sorption and condensation. This model was rather simplified and only appropriate for multi-layered clothing as it was assumed that the temperature and moisture content in each clothing layer were uniform. Vafai and Sarkar [6] first modeled the transient heat and moisture transfer with condensation rigorously. For the first time, the interface between the dry and wet zones was found directly from the solution of the transient governing

* Corresponding author. Tel.: +852-2766-6472; fax: +852-2773-1432.
E-mail address: tcfanjt@inet.polyu.edu.hk (J. Fan).

0017-9310/02/$ - see front matter
PII: S0017-9310(02)00114-X

Nomenclature

C_a	water vapor concentration in the inter-fiber void space ($kg\,m^{-3}$)
C_a^*	saturated water vapor concentration in the inter-fiber void space ($kg\,m^{-3}$)
C_f	water vapor concentration in a fiber over its radius at a position of the fibrous batting at a certain time ($kg\,m^{-3}$)
C_v	effective volumetric heat capacity of the fibrous batting ($kJ\,m^{-3}\,K^{-1}$)
C_{v0}	volumetric heat capacity of the dry fibrous batting ($kJ\,m^{-3}\,K^{-1}$)
C_w	volumetric heat capacity of water ($kJ\,m^{-3}\,K^{-1}$)
D_a	diffusion coefficient of water vapor in the air ($m^2\,s^{-1}$)
D_f	disperse coefficient of moisture in the fiber ($m^2\,s^{-1}$)
D_l	disperse coefficient of free water in the fibrous batting ($m^2\,s^{-1}$)
E	the evaporation coefficient, dimensionless
E_i	surface emissivity of the lining fabrics ($i = 1$: inner lining; $i = 2$: outer lining)
F	total thermal radiation incident on a point (W) (i.e. R: travel to the right, L: travel to the left)
H_c	convective mass transfer coefficient ($m\,s^{-1}$)
H_T	convective thermal transfer coefficient ($kJ\,m^{-2}\,K^{-1}$)
k_e	effective thermal conductivity of the fibrous batting ($kJ\,m^{-1}\,K^{-1}$)
k_f	thermal conductivity of fiber ($kJ\,m^{-1}\,K^{-1}$)
k_a	thermal conductivity of air filling in the fabric batting ($kJ\,m^{-1}\,K^{-1}$)
k_w	thermal conductivity of water in the fabric batting ($kJ\,m^{-1}\,K^{-1}$)
L	thickness of the fabric batting (m)
M	the molecular weight of the evaporating substance, 18.0152 (g/mol) for water
p	pressure of water vapor in the inter-fiber void (Pa)
p_{sat}	saturation vapor pressure of water at absolute temperature T_s (Pa)
p'_{sat}	the saturated vapour pressure at the temperature T_v (Pa)
p_v	vapor pressure in vapor region at T_s (Pa)
r	radius of fibers (m)
R	the universal gas constant, 8.314471×10^7 ($J\,K^{-1}\,mol^{-1}$)
R_{ti}	resistance of direct heat transfer ($s\,m^{-1}$) (i.e. $i = 0$: inner fabric, $i = 1$: outer fabric)
R_{wi}	resistance of water vapor transfer ($s\,m^{-1}$) (i.e. $i = 0$: inner fabric, $i = 1$ outer fabric)
RH_i	relative humidity (%) (i.e. $i = 0$: surface next to human body, $i = 1$: surrounding air)
T_{bi}	temperature of the boundaries (K) (i.e. $i = 0$: surface next to human body, $i = 1$: surrounding air)
C_{ai}	moisture concentration at the boundaries (K) (i.e. $i = 0$: surface next to human body, $i = 1$: surrounding air)
T_s	temperature at the interface (K)
T_v	temperature in vapor region (K)
t	real time from change in conditions (s)
w_i	resistance to water vapor (i.e. $i = 0$: inner fabric, $i = 1$: outer fabric)
W_f	water content of the fibers in the fabric, $W_f = C_f/\rho$
W	water content of the fibrous batting
W_c	critical level of water content above which the liquid water becomes mobile
W_i	initial water content
x	distance (m)
ε	porosity of the fabric (ε = cubic volume of inter-fiber space/total cubic volume of fabric space)
λ	latent heat of (de)sorption or condensation of water vapor by the fibers ($kJ\,kg^{-1}$)
ρ	density of the fibers ($kg\,m^{-3}$)
τ	effective tortuosity of the fabric. The degree of bending or twist of the passage of moisture diffusion due to the bending or twist of fibers in the fibrous insulation. It normally changes between 1.0 and 1.2, depending on the fiber arrangements
β	radiative sorption constant
σ	Boltzmann constant
Γ	the rate of (de)sorption, condensation, freezing and/or evaporation ($kg\,s^{-1}\,m^{-3}$)

equations. In this work, the effects of boundary conditions, the Peclet and Lewis number on the condensation process is numerically analyzed. Later Vafai and Tien [7] extended the analysis to two-dimensional heat and mass transport accounting for phase change in a porous matrix. Tao et al. [4] first analyzed the frosting effect in an insulation slab by applying Vafai and Sarker's model to the case with temperature below the triple point of water. They [8] have also for the first time considered the hygroscopic effects of insulation materials in the modeling. Murata [9] first considered the falling of condensate under gravity and built the phenomena into his

steady-state model. The effect of condensates on the effective thermal conductivity and radiative heat transfer were for the first time considered in Fan et al.'s transient model [10] on condensation in porous media.

Although considerable work has been carried out in the past on heat and moisture transfer with phase change, the transient solution to the problem with mobile condensates has not been found. The present work is to extend the previous transient model [10] to take into account of the movement and evaporation of condensates, which was speculated to be the main cause of the large reduction in thermal insulation observed experimentally [5].

2. Mathematical model

We consider a physical system (i.e. a clothing assembly) consisting of a thin inner fabric layer close to human body, a thick porous fibrous batting and a thin outer fabric next to the cold environment as shown in Fig. 1. The following assumptions are made:

1. The porous fibrous batting is isotropic in fiber arrangement and material properties.
2. Volume changes of the fibers due to changing moisture and water content are neglected.
3. Local thermal equilibrium exists among all phases and as a consequence, only sublimation or ablimation is considered in the frozen region.
4. Convective heat transfer in the fibrous batting is negligible. This is justified based on the past experimental work on dry heat transfer in fibrous insulation [11].
5. The moisture content at the fiber surface is in sorptive equilibrium with that of the surrounding air.

Consider the heat and moisture transfer within the porous batting, based on the conservation of heat energy and applying the two-flux model of radiative heat transfer [10,11], at position x and time t, we have

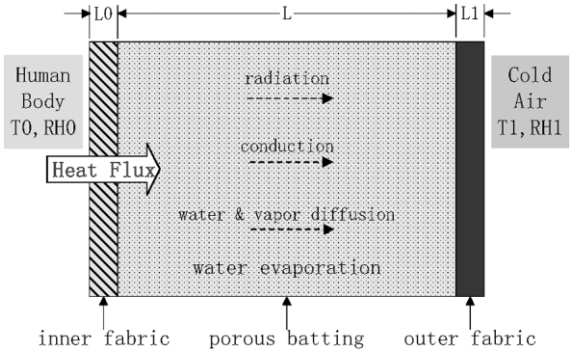

Fig. 1. Schematic diagram of the porous fabric assemblies.

$$C_v(x,t)\frac{\partial T}{\partial t} = \frac{\partial}{\partial x}\left(k_e(x,t)\frac{\partial T}{\partial x}\right) + \left(\frac{\partial F_L}{\partial x} - \frac{\partial F_R}{\partial x}\right) + \lambda(x,t)\Gamma(x,t) \quad (1)$$

where,

$$\frac{\partial F_L}{\partial x} = \beta F_L - \beta\sigma T^4(x,t)$$
$$\frac{\partial F_R}{\partial x} = -\beta F_R + \beta\sigma T^4(x,t)$$

According to mass conservation, moisture transfer in the inter-fiber void is governed by the following equation:

$$\varepsilon\frac{\partial C_a}{\partial t} = \frac{D_a\varepsilon}{\tau}\frac{\partial^2 C_a}{\partial x^2} - \Gamma(x,t) \quad (2)$$

The diffusion of free water in the porous batting is governed by:

$$\rho(1-\varepsilon)\frac{\partial(W - W_f)}{\partial t} = \rho(1-\varepsilon)D_l\frac{\partial^2(W - W_f)}{\partial x^2} + \Gamma(x,t) \quad (3)$$

where, $W_f(x,t) = C_f(x,t)/\rho$, which is the water absorbed within the fiber; W is the total water content including that absorbed by the fibers and on the fiber surface,

$$W(x,t) = \frac{1}{\rho}\int_0^t \Gamma(x,t)\,dt \quad (4)$$

$W - W_f$ is the water content on the fiber surface and is defined as the free water content. As the pore sizes in fibrous materials are generally small, the diffusion of liquid water is largely governed by capillary action. Since the capillary action is dependent on surface or fiber–water interface tension, which in turn relates to surface treatment and pore size, the dispersion coefficient, D_l in Eq. (3), is a function of the pore size and fiber surface treatment. However, as no empirical relation between D_l and the pore size and fiber surface treatment is available at the present, a constant value has been assumed in our model with reference to some previous work [14,15]. $D_l = 0$ when the condensate is immobile, which is the case when the water content is less than a critical value W_c, or when the free water is frozen. Eq. (3) only applies when $W > W_f$.

When the relative humidity is less than 100%, viz. there is no condensation, $\Gamma(x,t)$ is the rate of absorption or desorption, which may be determined according to the Fick's law of diffusion with a diffusion coefficient D_f dependent on the temperature and water content in fibers [10], viz.

$$\frac{\partial C_f'}{\partial t} = \frac{1}{r}\frac{\partial}{\partial r}\left(D_f\frac{\partial C_f'}{\partial r}\right) \quad (5)$$

where, r is the radius, C_f' is the volumetric moisture concentration in the fiber. The boundary condition for

Eq. (5) can be determined by assuming that the moisture concentration at the fiber surface $C'_f(x, R_f, t)$ (R_f is the radius of the fiber) is instantaneously in equilibrium with the surrounding air. Consequently, $C'_f(x, R_f, t)$ is a known function of the relative humidity of the surrounding air $\mathrm{RH}(x, t)$, i.e.,

$$C'_f(x, R_f, t) = f(\mathrm{RH}(x, t)) \tag{6}$$

The function, f, is a known empirical functional relationship, which can be found in textile textbooks in data or graphical form. With C'_f, the water content absorbed by the fibers W_f may be integrated by

$$W_f(x, t) = \{2/(\rho R_f^2)\} \int_0^{R_f} C'_f r \, dr \tag{7}$$

where, ρ is fiber density. After determining the fiber water content, the absorption rate $\Gamma(x, t)$ in the non-condensation region can then be calculated by:

$$\Gamma(x, t) = \Gamma_s(x, t) = \rho(1 - \varepsilon)\frac{\partial W_f(x, t)}{\partial t} \tag{8}$$

When the relative humidity reaches 100%, condensation takes place in addition to absorption. The water condensation rate $\Gamma_c(x, t)$ can be uniquely determined by the mass balance equation, i.e.

$$\Gamma_c(x, t) = \left(\frac{D_a}{\tau}\frac{\partial^2 C_a^*(x, t)}{\partial x^2} - \frac{\partial C_a^*(x, t)}{\partial t}\right)\varepsilon \tag{9}$$

where, $C_a^*(x, t) = 216.5 P_{sat} \times 10^{-6}/T(x, t)$.

When liquid water diffuses to the region where the relative humidity is below 100%, evaporation takes place. Many models had been proposed to determine water evaporation [12]. The model applied in the present study is expressed as follows:

$$\Gamma_e = E\sqrt{M/2\pi R}\left(P_{sat}/\sqrt{T_s} - P_v/\sqrt{T_v}\right) \tag{10}$$

Base on the definition of relative humidity, we have: $\mathrm{RH} = P_v/P'_{sat}$, therefore

$$P_v = \mathrm{RH} P'_{sat} \tag{11}$$

According to our third assumption, $T_v = T_s$, therefore

$$P'_{sat} = P_{sat} \tag{12}$$

Substitute P_v in Eq. (10) with Eq. (11), and then substitute P'_{sat} with P_{sat}, we get:

$$\Gamma_e = E\sqrt{M/2\pi R}(1 - \mathrm{RH})P_{sat}/\sqrt{T_s} \tag{13}$$

The effective thermal conductivity in Eq. (1) is calculated by

$$k_e = \varepsilon k_a + (1 - \varepsilon)(k_f + w k_w) \tag{14}$$

and the effective volumetric heat capacity of the fibrous batting is calculated by

$$C_v = C_{v0} + W C_w. \tag{15}$$

The boundary conditions to main differential equations (1) and (2) are the same as those reported previously [10]. Consider the conductive heat transfer at the interface between the inner thin fabric and the fibrous batting and that between the outer thin fabric and the fibrous batting, we have

$$\begin{aligned} k_e(x, t)\frac{dT^{n+1}(x)}{dx}\Big|_{x=0} &= \frac{T_0^{n+1} - T_{b0}}{R_0} \\ k_e(x, t)\frac{dT^{n+1}(x)}{dx}\Big|_{x=L} &= \frac{T_{b1} - T_N^{n+1}}{R_1 + 1/H_T} \end{aligned} \tag{16}$$

Consider the moisture diffusion at the interface between the inner thin fabric and the fibrous batting and that between the outer thin fabric and the fibrous batting, we have

$$\begin{aligned} D_a\varepsilon\frac{\partial C_a^{n+1}}{\partial x}\Big|_{x=0} &= \frac{C_{a0}^{n+1} - C_{ab0}}{w_0} \\ D_a\varepsilon\frac{\partial C_a^{n+1}}{\partial x}\Big|_{x=L} &= \frac{C_{ab1} - C_{a1}^{n+1}}{w_1 + 1/H_c} \end{aligned} \tag{17}$$

Consider the radiative heat transfer at the interface between the inner thin fabric and the fibrous batting and that between the outer thin fabric and the fibrous batting, we have

$$\begin{aligned} (1 - e_1)F_L(0, t) + e_1\sigma T^4(0, t) &= F_R(0, t) \\ (1 - e_1)F_R(L, t) + e_2\sigma T^4(L, t) &= F_L(0, t) \end{aligned} \tag{18}$$

3. Numerical computation

The differential equations in the above section were solved by the implicit finite difference method, with assumed initial conditions simulating different practical circumstances. The computational procedure was such that, at each time step and each position, the computed vapor concentration $C_a(x, t)$ was compared with the saturation vapor concentration $C_a^*(T(x, t))$ at the corresponding temperature. If the calculated vapor concentration was greater than, or equal to, the saturation one, condensation takes place, and $C_a(x, t)$ was then set to $C_a^*(T(x, t))$. In the condensation region, if the temperature is above 0 °C, it is a wet region; if the temperature is below 0 °C, it is a freezing region. The condensed water content was calculated by Eq. (9). At each time step and position, the free water content is checked, if $W > W_f$, Eq. (13) was used to calculate the rate of evaporation and Eq. (3) was used to calculate the free water diffusion. The liquid water diffusivity D_l will initially be set to be zero as there is no liquid movement at the start. At each time step and position, the calculated water content W was also compared with the critical water content W_c. If W was greater than W_c and the temperature was greater than 0 °C, D_l will be set to $D_l(W)$. With the new water

content, the effective thermal conductivity $k(x,t)$ was updated at each position and time step.

4. Analysis and verification of the model

Farnworth [5] reported qualitatively based on his experimental observation that, heat flux through wet fibrous batting was 3–5 times as much as that through dry batting. This dramatic increase in heat flux must be caused, he believed, by the extra heat transport due to the evaporation and diffusion of water vapor, since the increase in conductive heat transport due to the increased water content could only explain for an increase of 10% or 20%.

The new model proposed in this paper and the old model reported previously [10] were both applied to calculate the heat flux through an initially dry and an initially wet batting to see whether the inclusion of evaporation and liquid water movement in the new model can better explain the experimental observation by Farnworth [5]. The parameters used in this calculation are listed in Table 1. The results are plotted in Fig. 2. As can be seen, when the fibrous batting is initially dry, the heat flux predicted by the new model and that by the old model are very similar, indicating that evaporation and movement of liquid water considered in the new model have only small effect on the insulation property of the batting. However, when the initial water content is 50%, simulating a initially wet batting, the heat flux predicted by the new model is about 3 times of that by the old model, which indicates that evaporation and movement of liquid water in the batting are very important mechanism accounting for the dramatic increase in heat flux. The calculated results are in agreement with Farnworth's observation.

To better understand the mechanism of the phenomena, change of water content distribution with time predicted by the new model was plotted in Fig. 3 for the initially dry batting and in Fig. 4 for the initially wet batting, respectively. As can be seen, when the batting is initially dry the accumulation of condensed water is slow even under the cold condition of −20 °C. The condensed

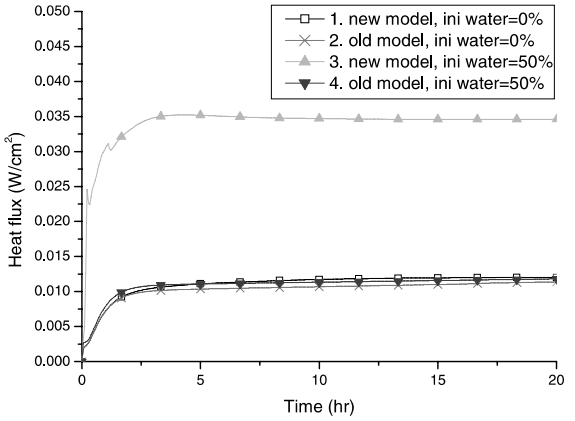

Fig. 2. Predicted heat flux for an initially dry and wet batting.

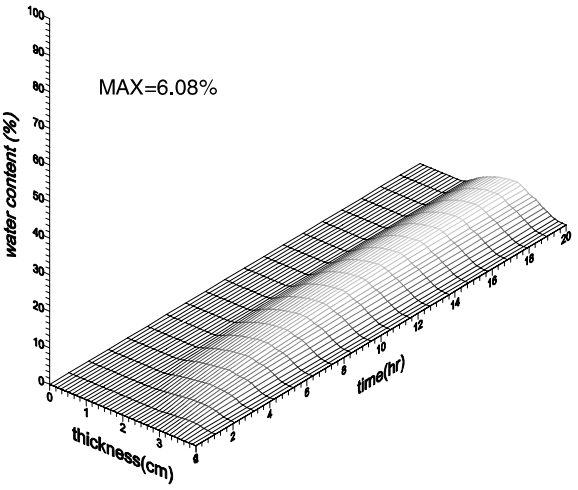

Fig. 3. Change of water content distribution with time in batting (new model).

Table 1
Parameters used in the calculation

ρ	λ			ε	τ	k_a	k_f
	Dry region	Wet region	Freezing region				
910.0	2522.0	2260.0	2593.0	0.87	1.2	0.025	0.1
k_w	β	D_a	D_f	D_l	C_{v0}	C_{w0}	E
0.57	8	2.5×10^{-5}	1.3×10^{-13}	2.5×10^{-9}	1715.0	4200.0	4.0×10^{-3}
W_c	e_1	e_2	σ	L	R_{w0}	R_{w1}	R_{t0}
0.5	0.9	0.9	5.672×10^{-12}	0.04	0.1	0.1	0.3
R_{t0}	RH_0	RH_1	T_{b0}	T_{b1}	r		
0.3	96%	90%	306 (33 °C)	253 (−20 °C)	1.03×10^{-5}		

Note: The fibrous batting was assumed to be made of polypropylene, which is hydrophobic in nature.

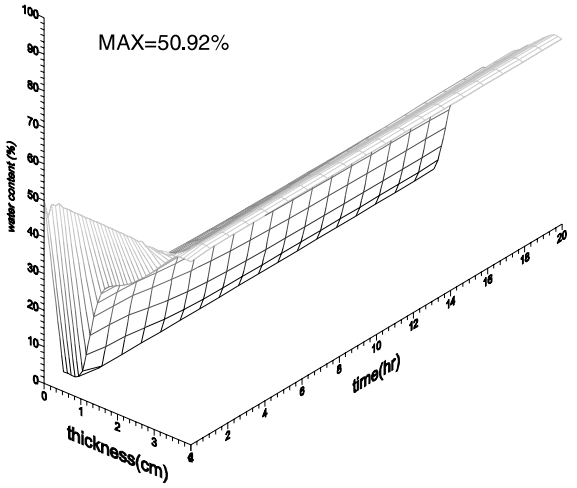

Fig. 4. Change of water content distribution with time in batting (new model).

water may diffuse to areas having lower water content and re-evaporate, resulting a rather flat water content distribution as shown in Fig. 3. However, the situation is very different for an initially wet batting. In this case, the water content in the inner region (i.e. close to the warm human body) reduces very quickly due to evaporation and the released moisture is diffused towards outer (or cold) region, where it is re-condensed. The condensed, but unfrozen (liquid) water in the outer region may move back to the inner warm region by liquid water diffusion and get re-evaporated in the inner region. The evaporation, moisture diffusion, condensation and liquid water movement create a cyclic effect, which greatly increases the heat flux through the system.

The model was also used to fit the experimental results of a drying test carried out by Farnworth [5]. In this test, a 13 mm thick polyester batting of 1.3% fiber volume (230 g/m^2), having an initial water content of 150%, was contained in a polyester mesh within a cylindrical holder (There was a 5 mm hole drilled through the holder to permit the exchange of water or moisture). Similar to polypropylene, polyester is also hydrophobic in nature. The assembly was prepared and placed on a hot plate controlled at 35 °C in an atmosphere of 22 °C and 30% RH. In the theoretical calculation, some parameters listed in Table 1 were adjusted to reflect the experimental condition. The value of adjusted parameters are listed in Table 2.

Fig. 5 compares the calculated results using our model with the experimental ones. The theoretically predicted results matches well with the experimental ones in trend. The generally lower heat loss may be due to the fact that additional heat energy was required in the experiment to dry off the water on the holder and absorbed by the polyester mesh.

Table 2
Value of the adjusted parameters

ρ	ε	L	T_{b0}	T_{b1}	RH_1	Initial water
1361.0	0.987	0.013	308 (35 °C)	295 (−22 °C)	30%	150%

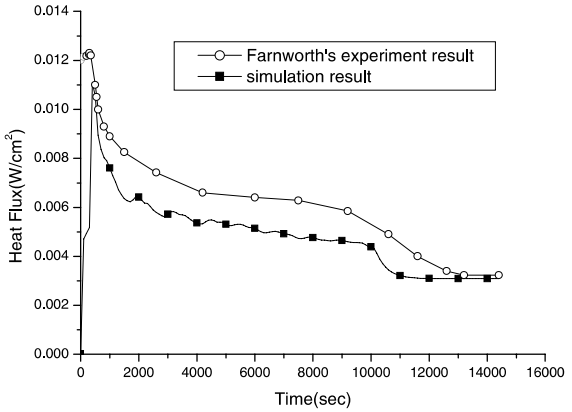

Fig. 5. Heat flux comparison between experiment result and simulated result.

5. Simulation results and discussion

The thermal insulation property of fibrous systems is very important to cold protection. In order to optimize the thermal insulation, numerical simulation was carried out to better understand the effects of various material and environmental parameters on the heat loss from the human body. In the simulation, one parameter was changed, but the rest kept constant as in Table 1.

5.1. Effect of initial water content

Figs. 6 and 7 show the effect of initial water content of the clothing assembly on the heat flux from the human body and the temperature distribution at the 20th hour, respectively, when the surrounding temperature is −20 °C. In general, heat flux is stabilized after about 5 h irrespective of the initial water content, reaching a quasi-steady-state. The temperature distribution at 20th hour is very different for clothing assemblies with different initial water content. As shown in Fig. 8, the effect of initial water content on the heat flux at 20th hour (representing the quasi-steady-state) is related to the surrounding temperature. When the surrounding temperature is 20 °C, the effect is very small. However, the heat flux increases greatly with the increase of initial water content when the surrounding temperature is −20 °C. Based on this analysis, therefore,

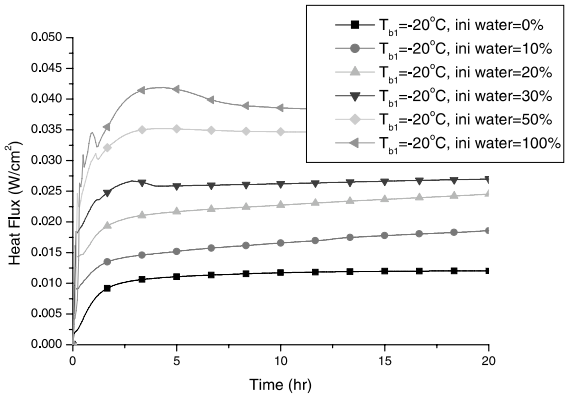

Fig. 6. Change of heat flux with time under different initial water content.

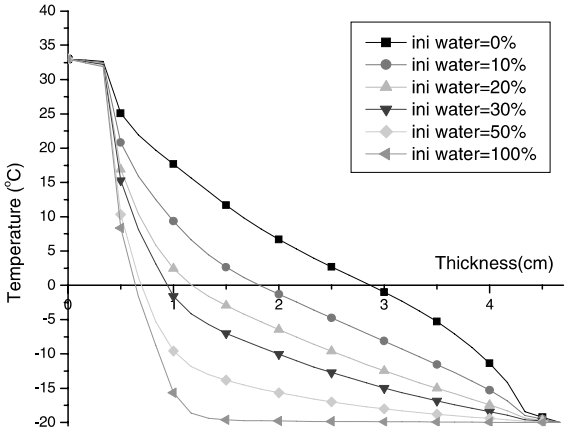

Fig. 7. Temperature distribution across the width at 20th hour when surrounding temperature is −20 °C.

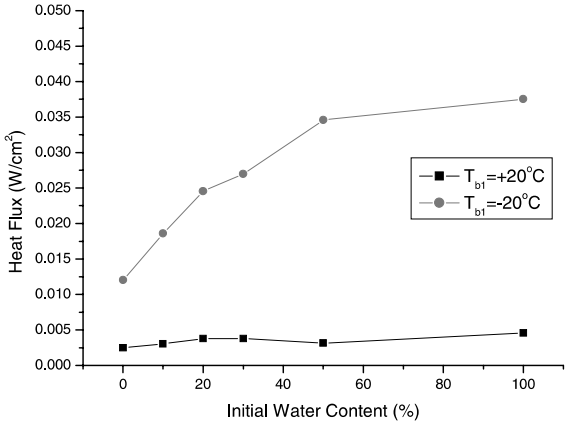

Fig. 8. Change of heat flux with initial water content at 20th hour under two surrounding temperatures.

it is important to keep the clothing dry in the cold weather to maintain its thermal insulation property.

When surrounding temperature is as low as −20 °C, affection of initial water on temperature distribution is also great. Fig. 15 shows the change of temperature with time of the central point of batting under different initial water content, and Fig. 16 shows the section temperature distribution of the clothing assemblies under different initial water content after 20 h. All the changes are quite great.

5.2. Effect of surrounding temperature

Figs. 9 and 10 shows the effect of surrounding temperature on the heat flux. As understood intuitively, the lower the surrounding temperature the greater the heat flux (more heat loss from the human body). When the surrounding temperature is equal to the body skin temperature of 33 °C, heat loss from human body only takes place in the initial 2 h and thereafter there is no

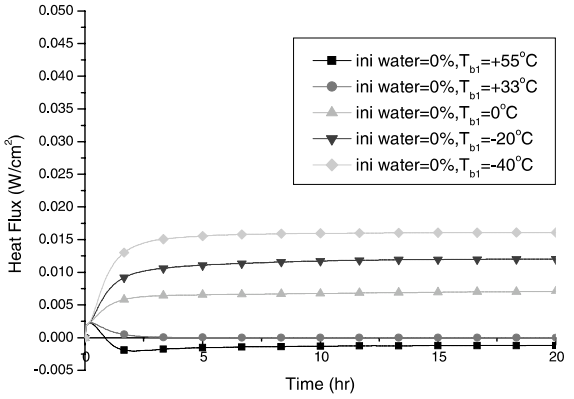

Fig. 9. Change of heat flux with time under different surrounding temperature.

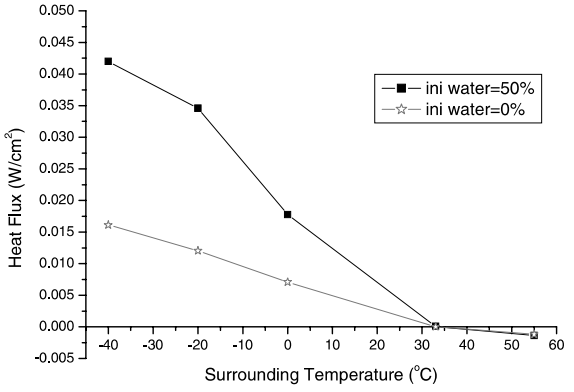

Fig. 10. Change of heat flux with surrounding temperature at 20th hour.

heat exchange between the human body and the environment. When the surrounding temperature is greater than 33 °C, the heat flux is negative after about 0.5 h. As indicated by Fig. 10, the effect of surrounding temperature is coupled by the initial water content. The higher the initial water content, the greater the effect of surrounding temperature. Note that the slopes of the curves in Fig. 10 when the surrounding temperature is below 33 °C (skin temperature) are very different those when surrounding temperature is above 33 °C. It may be concluded that the thermal insulation property of a clothing assembly for preventing cold surrounding is very different from that for preventing the hot whether surrounding, when evaporation and diffusion of water vapour takes place. The distribution of water content is also very different when the surrounding is hotter than the human body. As shown in Fig. 11, condensation takes place in the inner region close to the human body.

5.3. Effect of the thickness of fibrous batting

Figs. 12 and 13 shows the effect of the thickness of the fibrous batting on the heat flux from the human body. The results are in general agreement with the common sense that, the thicker the fibrous batting, the warmer (i.e. less heat flux) it is. However, the results showed that such effect was not linear. That is, the increase in the thickness of batting has greater effect on the insulation of the thinner batting than on a thicker batting. In other words, for an already thick clothing assembly (say more than 4 cm), a further increase in the thickness will only result in a small increase in the thermal insulation. It can also be seen from Fig. 13 that the effect of thickness of batting on thermal insulation is more pronounced at lower surrounding temperature.

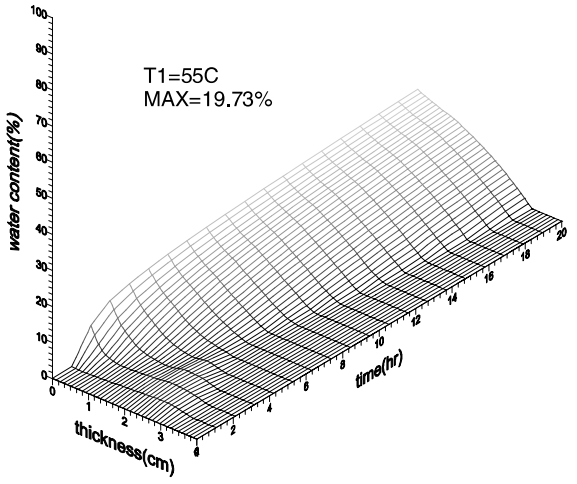

Fig. 11. Change of water content distribution with time when surrounding temperature is 55 °C.

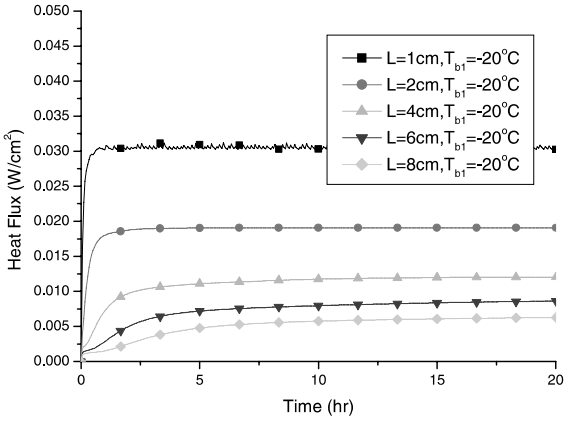

Fig. 12. Change of heat flux with time for different thickness of battings.

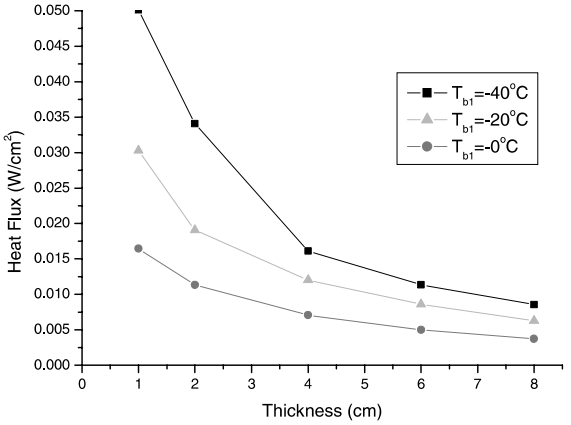

Fig. 13. Change of heat flux with batting thickness at 20th hour.

5.4. Effect of the breathability of inner lining

Both inner and outer lining fabrics' moisture transfer resistance are calculated and compared (w_0: inner; w_1: outer). Fig. 14 indicates that the resistance of moisture transfer has smaller affection on heat preservation property than previous studied parameters although heat preservation property do increase with the decrease of w_1 or increase of w_0. When the resistance value is bigger than 20 s/cm, almost no heat loss change comes from the resistance change.

5.5. Effect of the thermal conductivity of fiber

The effect of the thermal conductivity on the heat flux is shown in Figs. 15 and 16. It is well known, when there

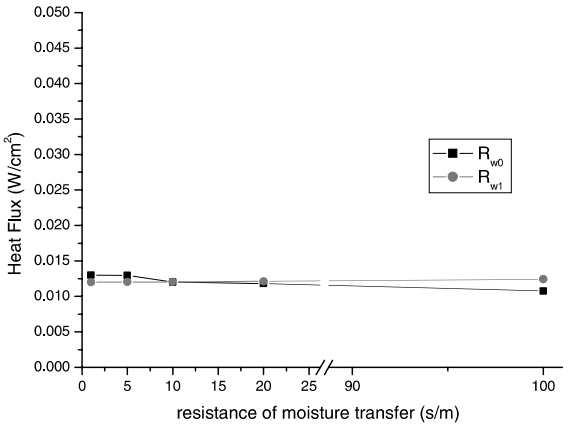

Fig. 14. Change of heat flux with resistance of moisture transfer in inner lining at 20th hour.

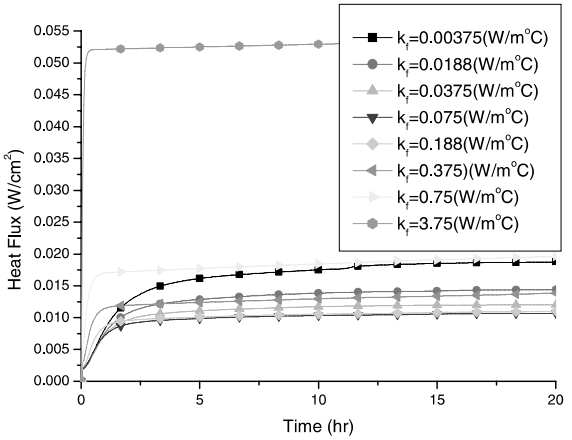

Fig. 15. Change of heat flux with time for fibers having different thermal conductivity.

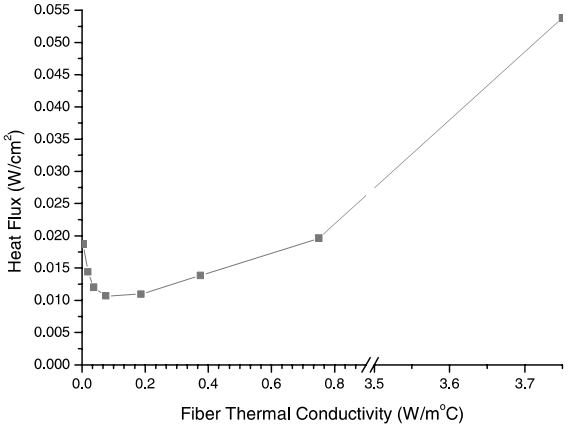

Fig. 16. Effect of fiber thermal conductivity on heat flux at 20th hour.

is only dry heat transfer, that the greater the fiber thermal conductivity, the greater the heat flux through the fibrous batting. However, when there is water vapor diffusion, phase change and movement of liquid condensates, as indicated by Fig. 16, heat flux reduces with increasing fiber thermal conductivity, k_f, when k_f is less than 1×10^{-3} W/cm °C. For k_f is greater than 1×10^{-3} W/cm °C, heat flux increases with increasing k_f.

Figs. 17–19 show how the distribution of condensed water content varies with k_f (i.e., fiber thermal conductivity). When the fiber thermal conductivity is very low at 1.88×10^{-4} W/cm °C, the condensed water is wide spread and the maximum water content is the lowest. When the fiber thermal conductivity is greater at 7.5×10^{-4} W/cm °C (see Fig. 18) and 7.5×10^{-3} W/cm °C (see Fig. 19), the wet zone gets closer to the outer region, and there is a value of maximum water content.

From Fig. 16, when the environment is at −20 °C, the optimum fiber thermal conductivity is in the range between 1 and 2×10^{-3} W/cm °C, which is the range of

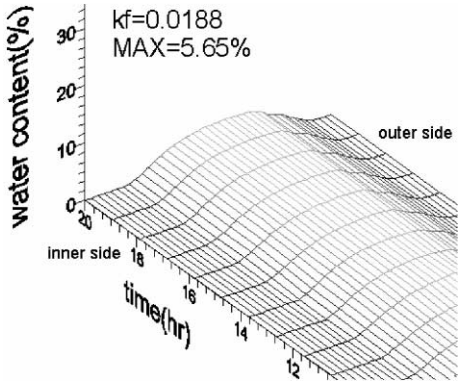

Fig. 17. Water content distribution for $k_f = 0.0188$ W/m °C.

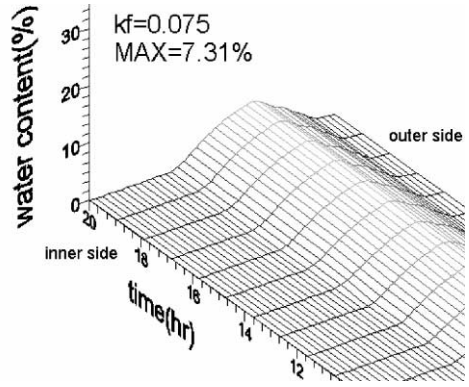

Fig. 18. Water content distribution for $k_f = 0.075$ W/m °C.

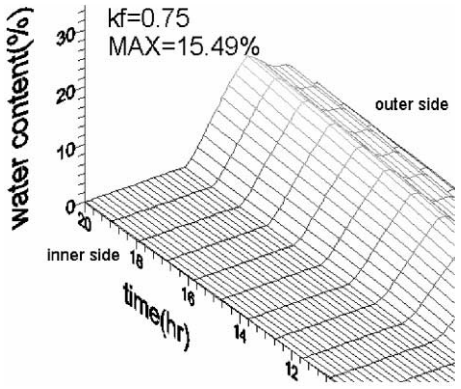

Fig. 19. Water content distribution for $k_f = 0.75$ W/m °C.

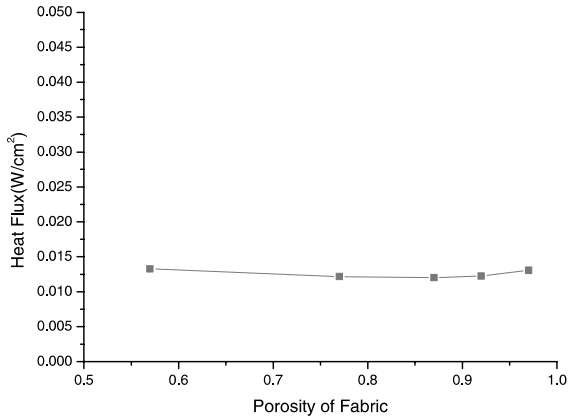

Fig. 20. Change of heat flux with batting's porosity at 20th hour.

most of textile fibers [13]. It can be said that textile fibers are very good insulators of cold weather.

5.6. The effect of the porosity of fibrous batting

Higher porosity means more air void and less fibers in the batting. From Fig. 20, we can see that the effect of the porosity in general is very small. Specifically, when the porosity increases from 0.57 to 0.87, heat flux reduces and when the porosity increases further from 0.87, the heat flux increases. This may be due to the two conflicting effects of porosity on heat flux. The first one is that the increase in porosity reduces the effective thermal conductivity and hence the heat flux. The second one is that the increase in porosity reduces the water vapor resistance and hence increases the moisture diffusion. Therefore, heat flux will increase. Fig. 20 tells that there may exist an optimal porosity value that brings optimum thermal insulation property when other parameters are unchanged.

6. Conclusions

Water evaporation and movement in porous media are important phenomena, which can greatly affect the coupled heat and moisture transfer. In our work, such phenomena have been incorporated into a dynamic model for the first time. Based on the comparison between the theoretical and experimental results, the proposed model is believed to be appropriate for porous clothing assemblies used in cold weather conditions. The model may be further extended to other porous media.

Based on numerical results of the proposed model, it was found that initial water content, surrounding temperature and batting thickness are three key factors influencing the heat flux through the clothing assemblies. Other parameters, such as the water vapor resistance of the outer and inner lining fabric, thermal conductivity of fiber and porosity of porous batting were found to have only small effects.

Acknowledgements

The authors would like to thank the Research Grant Committee of the Hong Kong University Grant Council for funding the project.

References

[1] Y. Ogniewicz, C.L. Tien, Analysis of condensation in porous insulation, J. Heat Mass Transfer 24 (1981) 421–429.
[2] S. Motakef, M.A. El-Masri, Simultaneous heat and mass transfer with phase change in a porous slab, J. Heat Mass Transfer 29 (10) (1986) 1503–1512.
[3] A.P. Shapiro, S. Motakef, Unsteady heat and mass transfer with phase change in porous slab: analytical solutions and experimental results, J. Heat Mass Transfer 33 (1) (1990) 163–173.
[4] Y.X. Tao, R.W. Besant, Rezkallah, Unsteady heat and mass transfer with phase changes in an insulation slab: frosting effects, Int. J. Heat Mass Transfer 34 (7) (1991) 1593–1603.
[5] B. Farnworth, A numerical model of the combined diffusion of heat and water vapor through clothing, Tex. Res. J. 56 (11) (1986) 653–665.
[6] K. Vafai, S. Sarkar, Condensation effects in a fibrous insulation slab, J. Heat Transfer 108 (8) (1986) 667–675.
[7] K. Vafai, H.C. Tien, A numerical investigation of phase change effects in porous materials, Int. J. Heat Mass Transfer 32 (7) (1989) 1261–1277.
[8] Y.X. Tao, R.W. Besant, Rezkallah, The transient thermal response of a glass–fiber insulation slab with hygroscopic

effects, Int. J. Heat Mass Transfer 35 (5) (1992) 1155–1167.
[9] K. Murata, Heat and mass transfer with condensation in a fibrous insulation slab bounded on one side by a cold surface, Int. J. Heat Mass Transfer 38 (17) (1995) 3253–3262.
[10] J. Fan, Z. Luo, Y. Li, Heat and moisture transfer with sorption and condensation in porous clothing assemblies and numerical simulation, Int. J. Heat Mass Transfer 43 (2000) 2989–3000.
[11] B. Farnworth, Mechanics of heat flow through clothing insulation, Tex. Res. J. (1983) 717–725.
[12] Jones, E. Frank, Evaporation of Water with Emphasis on Application and Measurements, Lewis Publishers, Michigan, USA, 1992, pp. 25–43.
[13] A. Rae, R. Bruce (Eds.), The Wira Textile Data Book, Wira, 1973.
[14] A.V. Anisimov, Water diffusion in biological porous systems: A NMR approach, Magn. Reson. Imaging 16 (5/6) (1998) 565–568.
[15] Yoshito Nakashima, The use of X-ray CT to measure diffusion coefficients of heavy ions in water-saturated porous media, Eng. Geol. 56 (2000) 11–17.